Spring 3-2005

The Effect of Dose Rate on the Crystalline Lamellar Thickness Distribution in Gamma Radiation of UHMWPE

Jason B. Walker
University of Tennessee - Knoxville

Submitted to the Journal of Nuclear Methods and Instruments B

The Effect of Dose Rate on the Crystalline Lamellar Thickness Distribution in Gamma-Radiation of UHMWPE

C.P. Stephens[a], R.S. Benson[*a], Ma. Esther Martinez-Pardo[b], E.D. Barker[a], J.B. Walker[c], and T.P. Stephens[a]

[a] *University of Tennessee, Materials Science and Engineering, 434 Dougherty Engineering Building, Knoxville, Tennessee, TN 37996-2200, USA*
[b] *National Institute for Nuclear Research, C.P. 52045, Mexico*
[c] *University of Tennessee, Chemical Engineering, 416 Dougherty Engineering Building, Knoxville, Tennessee, TN 37996-2200, USA*

Submitted to the Journal of Nuclear Methods and Instruments B

The Effect of Dose Rate on the Crystalline Lamellar Thickness Distribution in Gamma-Radiation of UHMWPE

C.P. Stephens[a], R.S. Benson[*a], Ma. Esther Martinez-Pardo[b], E.D. Barker[a], J.B. Walker[c], T.P. Stephens[a]

[a] *University of Tennessee, Materials Science and Engineering, 434 Dougherty Engineering Building, Knoxville, Tennessee, TN 37996-2200, USA*

[b] *National Institute for Nuclear Research, C.P. 52045, Mexico*

[c] *University of Tennessee, Chemical Engineering, 416 Dougherty Engineering Building, Knoxville, Tennessee, TN 37996-2200, USA*

[*]Corresponding author: University of Tennessee, Materials Science and Engineering, 434 Dougherty Engineering Building, Knoxville, Tennessee, TN 37996-2200, USA; E-mail: rbenson1@utk.edu

Abstract

This study develops a connection between radiation integral dose, dose rate and crystallite thickness. Samples are irradiated at an integral dose of 75 and 150 kGy and at a dose rate of 0.25 and 2.9 kGy/hr. The degree of crystallinity and lamellar thickness distributions are determined from DSC. DSC shows the existence of two discrete crystalline lamellar distributions that are highly effected by irradiation protocol. It is also shown that the depth of the material from the surface also plays a role in the lamellar distribution. SAXS is then used to confirm the approximate range of lamellar thicknesses and the existence of two discrete crystallites.

1. Introduction

Ultra High Molecular Weight Polyethylene (UHMWPE) established itself as the wearing surface for the hip and knee artificial joint in 1967, after being introduced by Sir John Charnley to the

orthopedic community as a highly chemical resistant, low wear, and biocompatible material [1]. There is still a driving force for research in the area of γ-radiation of UHMWPE due to the need for improved performance of weight-bearing artificial joints. Although a large collection of research has been established, there is still a missing linkage between the true radiation conditions, specifically integral dose and dose rate, and the depth sensitive morphology of the polymer. Many articles have been published trying to elucidate the connection between radiation dose and morphological changes, however this study will be the first contemporary effort to allow the radiation dose rate ($\dot{\gamma}$) to be treated as a variable [1-8]. This study will investigate the effect of radiation applied at a $\dot{\gamma}$ of 0.25 kGy/hr and 2.9 kGy/hr at an integral dose (γ) of 75 kGy and 150 kGy. Small-Angle X-Ray Scattering (SAXS) and Differential Scanning Calorimetry (DSC) are used in conjunction to develop an understanding of the morphological changes in the material with varying dose and dose rate.

2. Materials and Methods

2.1. Sample Preparation

UHMWPE samples are machined into discs with a diameter of 35 mm and a thickness of 6.35 mm from a rod of Tivar® 1000 produced by Poly Hi Solidor. The samples are then exposed to gamma irradiation from a ^{60}Co source at a $\dot{\gamma}$ of 0.25 (LDR) or 2.9 kGy hr^{-1} (HDR) for a γ of 75 or 150 kGy. Following radiation a 6.35 mm diameter cores are taken from the sample and sliced into 1 mm thick discs using a razor blade. These 1 mm thick discs are used for both DSC and SAXS experiments.

2.2. Differential Scanning Calorimeter (DSC)

2.2.1. Heating Rate of 10 °C/ min

A 1 mm thick disc from the top and center of each sample is held at 25°C for 5 minutes, heated from 25°C to 200°C at 10 °C/min, cooled from 200°C to 25°C at 20 °C/min, and then heated again from 25°C to 200°C at 10 °C/min in a Mettler Toledo DSC 821^e. The degree of crystallinity is determined from Equation 1, where the ΔH_{FUS} is the heat of fusion of the sample and ΔH^o_{FUS} is the heat of fusion for a 100% crystalline material taken to be 288 J/g [9, 10].

$$X_C = \frac{\Delta H_{FUS}}{\Delta H^o_{FUS}} \quad (1)$$

2.2.2. Heating Rate of 1 °C/ min

A 1 mm thick disc from the top and middle of each sample is held at 75°C for 10 minutes, heated from 75°C to 180°C at 1 °C/min. These slow rate experiments avoid the artificial increase of the T_m, seen in the 10 °C/min heating rate experiments, to values above the theoretical melting temperature of polyethylene assigned to infinite size crystals, T_m^o. Increase in melting temperature of UHMWPE has been cited by Zachariades and Logan [11, 12]. The anomaly is possible due to existence of the crystals in a microenvironment consisting of high degree of chain entanglement and/or cross-linking found in these irradiated UHMWPE samples. Following each DSC run melting temperature corrections are conducted using an Indium standard. The calculated thermal parameters are used to determine the probability density as a function of temperature as given by *f(T)*, Equation 2. Where ΔH_m is the heat of fusion per unit mass for the perfect crystal, P(T) is the DSC power output, ρ_c is the crystalline density, M is the sample mass, and α_m is the mass fraction crystallinity of the sample [13].

$$f(T)\,dT = \frac{1}{\alpha_m \Delta H_m} \frac{P(T)dT}{M\left(dT/dt\right)} \tag{2}$$

An apparent crystal thickness distribution is calculated from transferring f(T) into an equation dependent on *l*, the crystal thickness, Thompson equation, Equation 3, (as shown in Figure 1) and the weight distribution function of thickness, Equation 4 and 5, where σ_e is the basal surface energy, T_m^o is the melting temperature for an infinite crystal, and T_m is the melting temperature of the sample [13-15].

$$l = \frac{2\sigma_e 10^3}{\Delta H_m \rho_c \left(1 - \frac{T_m}{T_m^o}\right)} \quad , nm \tag{3}$$

$$g(l) = KP(T)\left(T_m^o - T\right)^2 \quad , nm^{-1} \tag{4}$$

$$K = \frac{\rho_c}{2\sigma_e T_m^o M \alpha_m 10^9 \left(dT/dt\right)} \tag{5}$$

The constant parameters for polyethylene are T_m^o=418.7 K, ΔH_m=288 kJ/kg, σ_e=90 mJ/m^2, and ρ_c=967 kg/m^3 and the sample dependent parameters are T_m in K, α_m, M in kg, dT/dt in K per second and P(T) in mW [13].

2.3. Small Angle X-Ray Scattering (SAXS)

SAXS is an analytical technique utilized to determine the long period and lamellae thickness of polymers. SAXS was performed on a Molecular Metrology Microsource instrument operating at 45 kV and 0.66 mA. Scattering experiments were conducted at both 0.5 m (q=0.0005 to 0.76 nm^{-1}) and 1.5 m (q=0.00017 to 0.255). The spliced data is next corrected for thermal density fluctuations using Ruland's method [16]. These values can then be implemented in a Lorenz plot of the intensity as a function of the scattering vector, q. The scattering vector itself can subsequently be replaced using equations 6 and 7,

$$L = \frac{2\pi}{q} \tag{6}$$

$$l = L * \alpha_{DSC(10^{o} C\,min^{-1})} \tag{7}$$

where L is the long period, l as the lamellar thickness in nanometers, and α_{DSC} as the percentage of crystallinity as determined by the DSC at a heating rate of 10 °C/ min [10, 16].

3. Results and Discussion

3.1. Differential Scanning Calorimeter (DSC)

3.1.1. Heating Rate of 10 °C/ min

The calculated degree of crystallinity from DSC summarized in Table 1, shows a difference between the top surface and the center of each sample, Figure 2. This difference between unirradiated samples (control) is attributed to machining effects, since after recrystallization and a second heating cycle the surface and the center of the control sample have the same degree of crystallinity. This fact in combination with the remaining difference between the center and surface of the irradiated samples leads to the idea of there being some fundamental morphological difference between the center and surface, post irradiation. There is also a significant difference between the top and center of the sample due to the free-radicals access to oxygen molecules (O_2). With an increase in radiation dose there is an increase in the amount of chain scission on the surface of the sample for both high (HDR) and low dose (LDR) rates, as seen by the increase in crystallinity shown in Figures 2. At HDR, a larger number of chain scissions and free radicals are produced, which leads to a greater possibility for interaction with oxygen and subsequent recrystallization, with an increase in the degree of crystallinity. In the second DSC run, Figure 3, shows the surface of the irradiated samples has a higher degree of crystallinity than the control surface and the center of the irradiated samples has a lower degree

of crystallinity than the center of the control sample. These results suggest a high degree of chain scissioning on the surface of the irradiated samples and crosslinking in the center of the irradiated samples. It can also be seen from Figure 3 that the crystallinity of the center of the samples decreases as a function of integral dose. In the second run, the center of the LDR sample showed lower crystallinity than the HDR sample, potentially due to a higher degree of crosslinking.

3.1.2. Heating Rate of 1 °C/ min

DSC experiments were conducted at a slower heating rate of 1 $^{\circ}Cmin^{-1}$ to enable the calculation of a probability distribution function for lamella thickness using Equations 2-5. The probability distribution for the center and surface of the sample is presented in Figure 4 and 7, respectively.

Center of Sample:

Figure 4 shows an increase in crystalline lamellar thickness distribution breadth with an increase in either radiation dose or dose rate, as seen by the linear increase in the tail value of the distribution, shown in Figure 5; the approximate maximum thickness based on the tail position is 35 nm for the control, 88 nm for the 75 kGy LDR, 94 nm for the 75 kGy HDR, 137 nm for the 150 kGy LDR, and 151 nm for the 150 kGy HDR. Figure 6, shows that the increases in crystalline lamellar thickness for the secondary peak is independent of dose rate until a integral dose greater than 75 kGy, where the HDR sample continues to slightly increase in lamellar thickness and the LDR sample slightly decreases in lamellar thickness.

Surface of Sample:

Figure 7 shows a non-linear increase in lamellar thickness at both the tail of the distribution and the second peak in the distribution. Figure 8, the breadth of the distribution, shows that the lamellar thickness increases independent of dose rate until an integral dose rate greater than 75

kGy, where the HDR sample decreases in thickness and the LDR sample continues to increase in thickness almost linearly. Figure 9, the value at the secondary peak, shows an increase in thickness that is independent of dose rate until a value greater than 75 kGy, where the HDR sample has a lower peak thickness than the LDR sample.

3.2. Small Angle X-Ray Scattering (SAXS)

SAXS crystallite distributions, $I*q^2$ vs. lamellar thickness plot, is deconvoluted using two Gaussian peaks and tabulated in Table 2. This simple analysis allows for a rough estimation of the lamellar thickness, but does not take into account model constraints, such as the shape of the crystals. These results indicate a bimodal crystal distribution and crystal thickness similar to those predicted in DSC. The DSC and SAXS lamellar thickness distributions shows two peak values, which agrees with SAXS experiments conducted by Premnath et. al in 1999 [8]. One difference between the results of Premnath and the results presented in this paper is that the second smaller crystal, only appearing after irradiation in Premnath's work, is resolved as a small shoulder in the control state and grows into well-distinguished peak under the influence of radiation.

4. Conclusions

UHMWPE shows a strong crystallite thickness dependence on both gamma integral dose and depth into the sample. At integral doses of 150 kGy UHMWPE shows a dependence on dose rate, as shown by both the degree of crystallinity changes and changes in the lamellar thickness distribution.

References

1. S.M. Kurtz, The UHMWPE Handbook, Elsevier Academic Press, San Diego, 2004.
2. R.S. Benson, C.P. Stephens, Ma. E. Martinez-Pardo, Journal of Applied Medical Polymers 6, 2 (2002).
3. O.K. Muratoglu, D.O. O'Connor, C.R. Bragdon, M. Jasty, W.H. Harris, in: Proc. 11th Conference of ESB, Toulouse, France 1998.
4. S. Kurtz, L. Pruitt, C. Jewett, J. Foulds, A. Edidin, Biomaterials (1990) 1449.
5. S. Kurtz, C. Muhlstein, A. Edidin., Journal of Biomedical Materials Research 52 (2000) 447.
6. S.M. Kurtz, O.K. Muratoglu, M. Evens, A.A. Edidin, Biomaterials 20 (1999) 1659.
7. G. Lewis, Biomaterials 22 (2001) 371.
8. V. Premnath, A. Bellare, E.W. Merrill, M. Jasty, W.H. Harris, Polymer 40 (1999) 2215.
9. H.F. Ferguson, D.J. Frurip, A.J. Pastor, L.M. Peerey, L.F. Whiting, Thermochimica Acta (2000) 363.
10. M.-H. Kim, Thesis in Materials Science and Engineering (1996) The University of Tennessee.
11. C.P. Stephens, in: Proc. Society of Plastics Engineers ANTEC, Nashville, Tennessee 2003.
12. A.E. Zachariades and J.A. Logan, Journal of Polymer Science B 21 (1983) 821.
13. B. Crist and F.M. Mirabella, Journal of Polymer Science B 37 (1999) 3131.
14. A.L. Valles-Llunch, L. Contat-Rodrigo, A. Riber-Greus, Journal of Applied Polymer Science 89 (2003) 3359.
15. J.T.E. Cook, P.G. Klein, I.M. Ward, A.A. Brian, D.F. Farrar, J. Rose, Polymer 41 (2000) 8615.

16. S.L. Schreiber, Thesis in Materials Science and Engineering (1998) The University of Tennessee.

List of Figures and Tables:

Figure 1: DSC Space Transformation

Table 1: Degree of Crystallinity from Differential Scanning Calorimetry

Figure 2: Degree of Crystallinity –First Run

Figure 3: Degree of Crystallinity-Second Run

Figure 4: Probability Distribution Based on DSC of Samples from the Middle Section

Figure 5: Breadth, Lamellar Thickness at the Tail, of the Center Lamellar Thickness Distribution (Figure 4)

Figure 6: Lamellar Thickness at the Second Peak (Crystal 2) of the Center Lamellar Thickness Distribution (Figure 4)

Figure 7: Probability Distribution Based on DSC of Samples from the Top

Figure 8: Breadth, Lamellar Thickness at the Tail, of the Surface Lamellar Thickness Distribution (Figure 6)

Figure 9: Lamellar Thickness at the Second Peak (Crystal 2) of the Surface Lamellar Thickness Distribution (Figure 6)

Table 2: SAXS Crystallite Peak Position, Determined by Deconvolution of the $I*q^2$ vs. Lamellar Thickness Plot

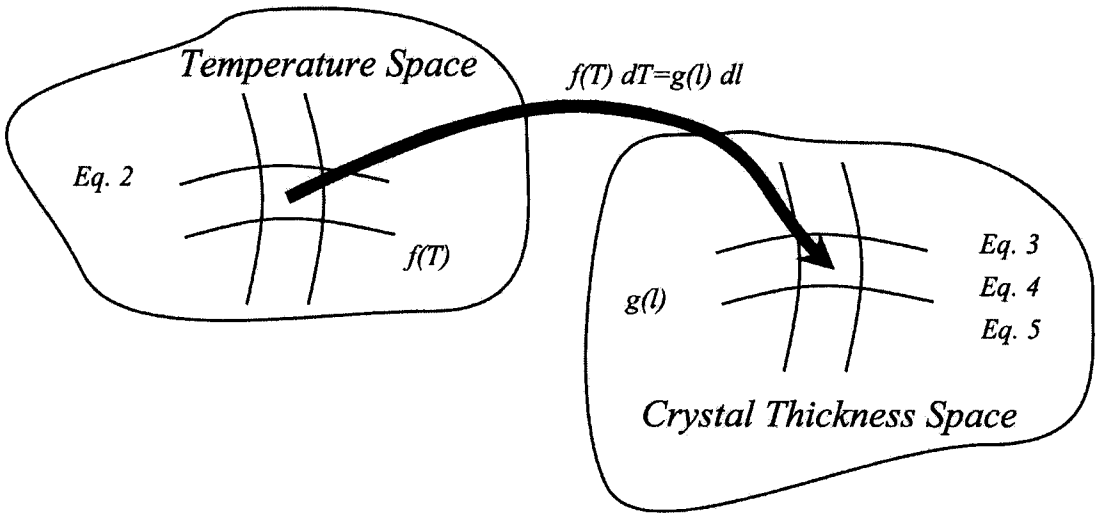

Figure 1

Table 1

Sample		Degree of Crystallinity[a] (%)	T_m (°C)[a]	Degree of Crystallinity[b] (%)
Control	Top	57.16 ± 0.31	139.45 ± 0.57	52.07 ± 0.64
	Middle	54.32 ± 0.21	138.50 ± 0.13	51.73 ± 1.20
75 kGy HDR	Top	64.27 ± 0.83	142.49 ± 0.72	55.35 ± 0.33
	Middle	61.61 ± 0.30	142.85 ± 1.33	52.66 ± 0.66
75 kGy LDR	Top	63.85 ± 1.92	142.20 ± 0.42	56.31 ± 3.08
	Middle	61.14 ± 1.40	143.02 ± 0.30	51.48 ± 1.12
150 kGy HDR	Top	66.07 ± 3.12	142.59 ± 0.42	56.13 ± 0.44
	Middle	59.86 ± 1.12	144.27 ± 0.89	50.37 ± 1.03
150 kGy LDR	Top	65.07 ± 0.50	142.98 ± 0.55	55.89 ± 1.28
	Middle	58.88 ± 0.68	144.91 ± 0.42	48.07 ± 0.42

a =first run; b= second run

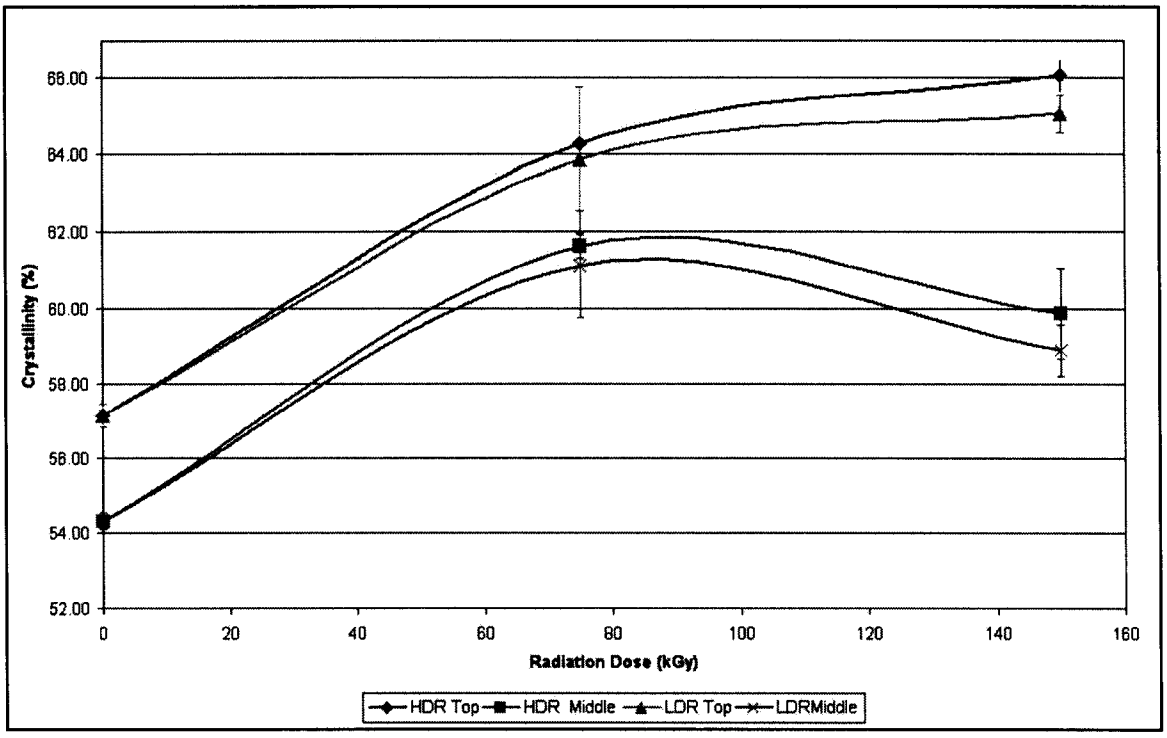

Figure 2

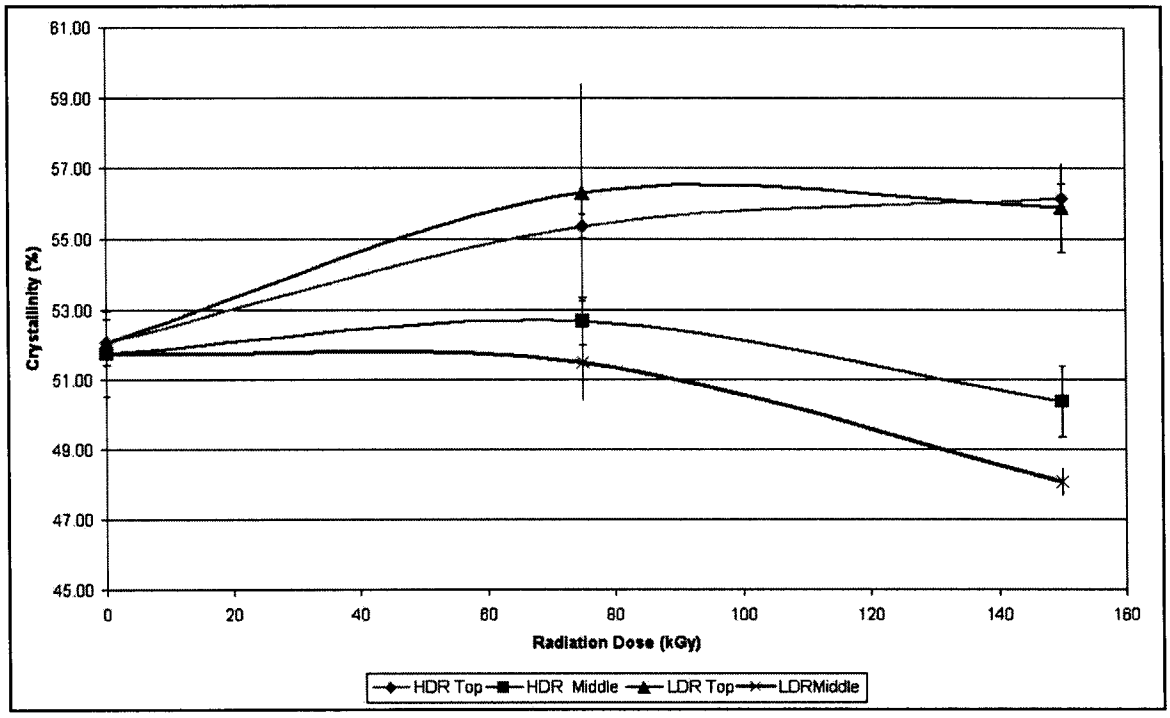

Figure 3

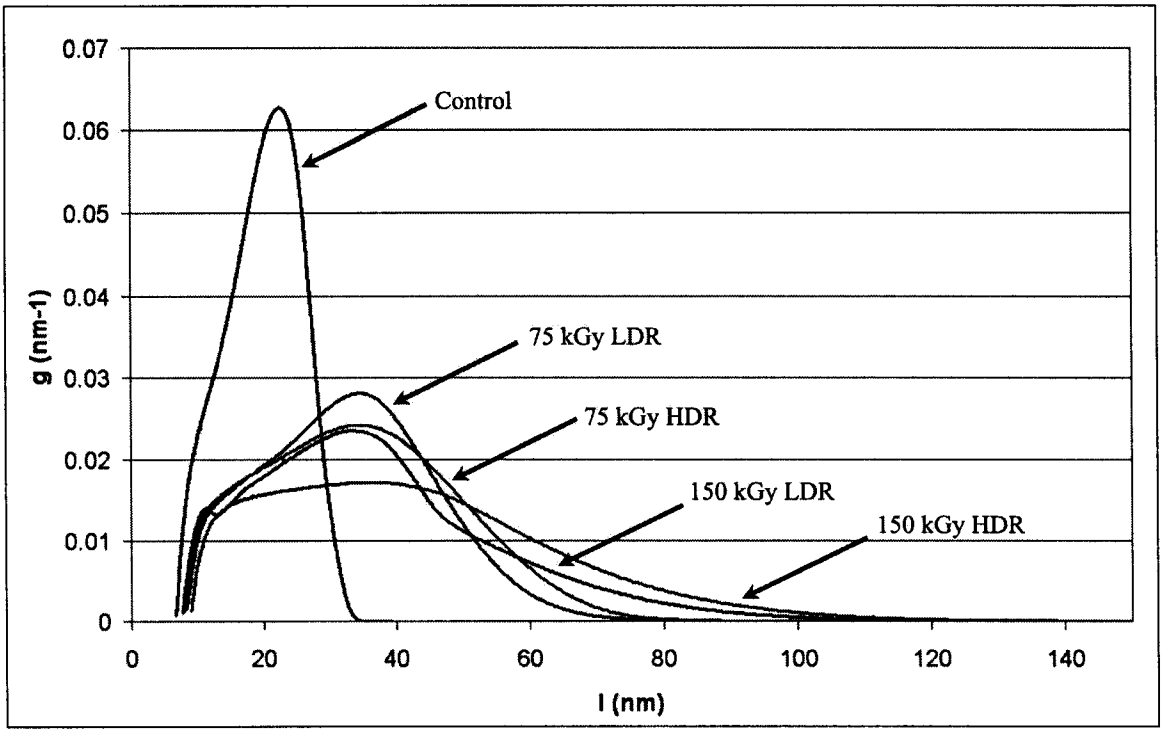

Figure 4

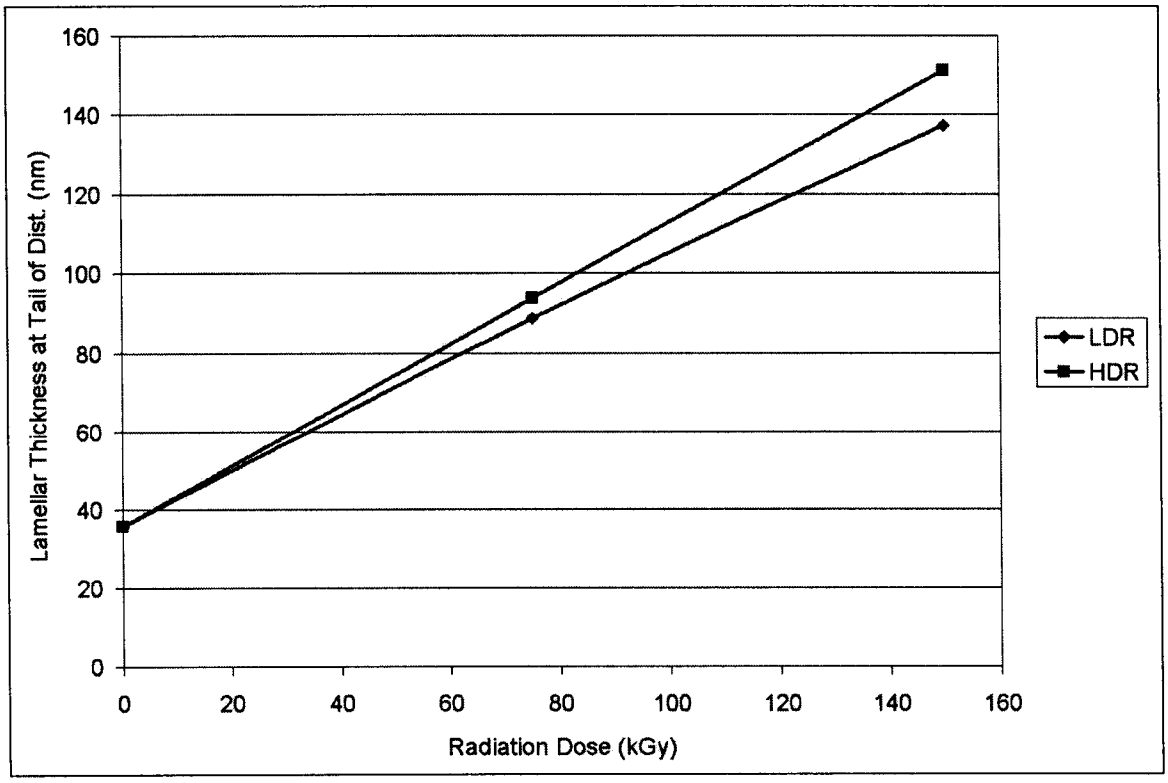

Figure 5

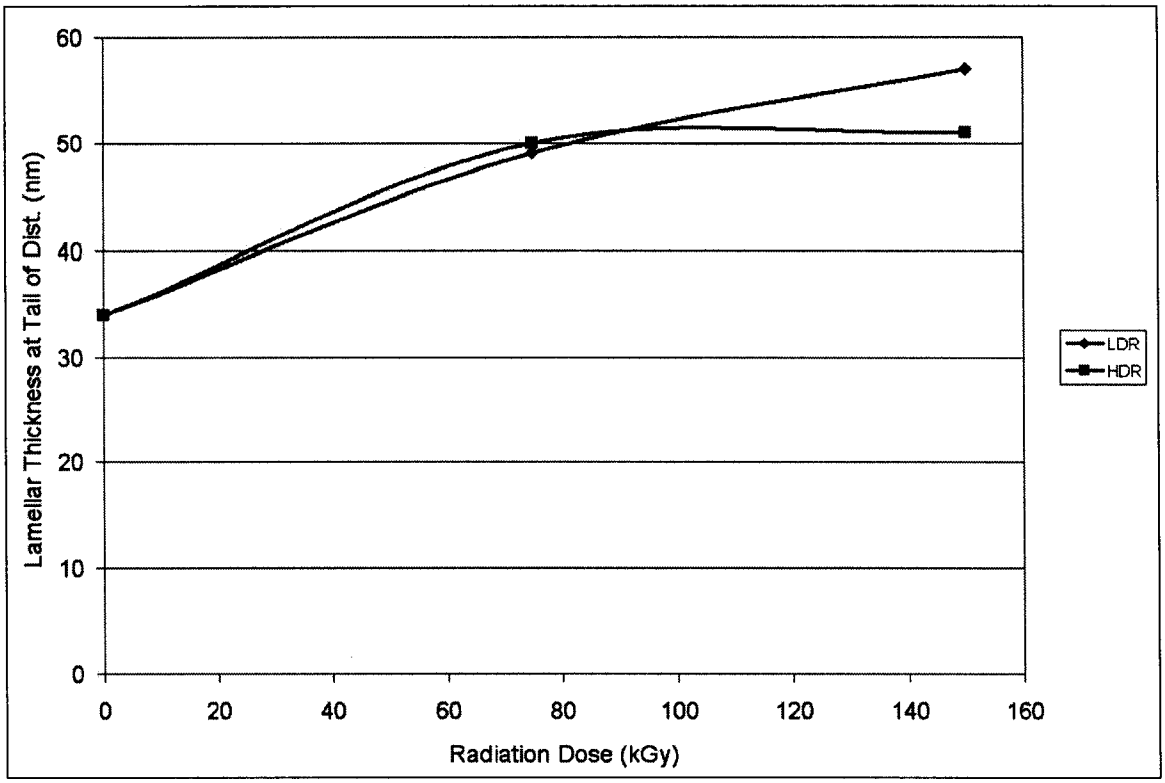

Figure 6

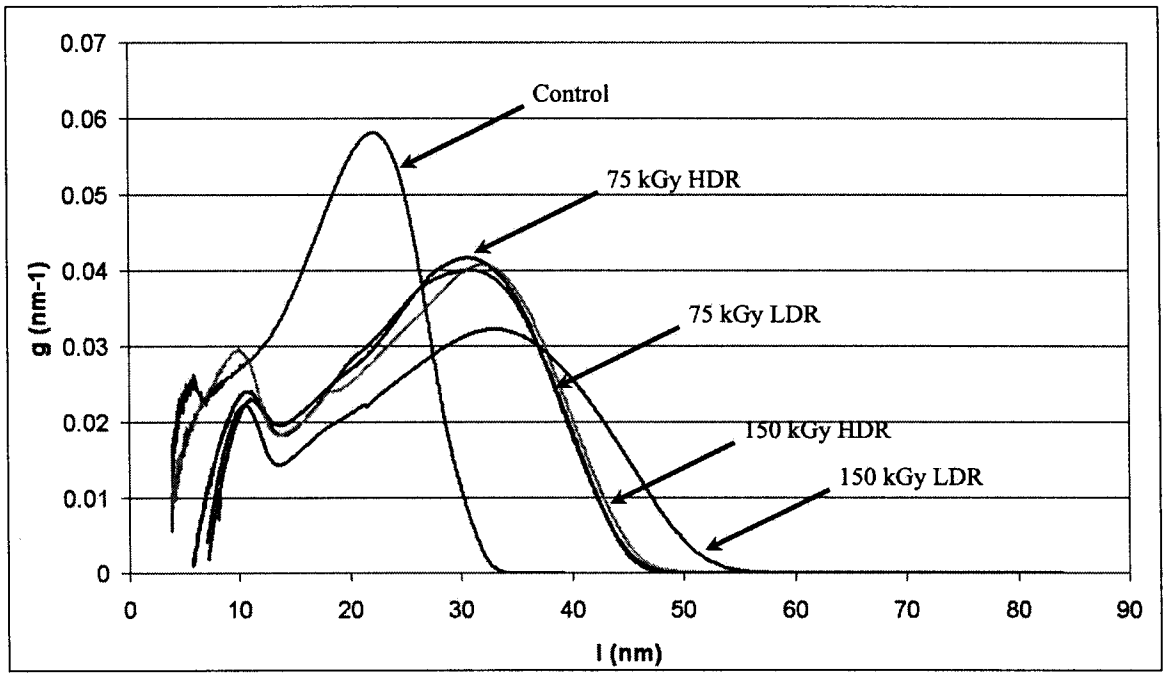

Figure 7

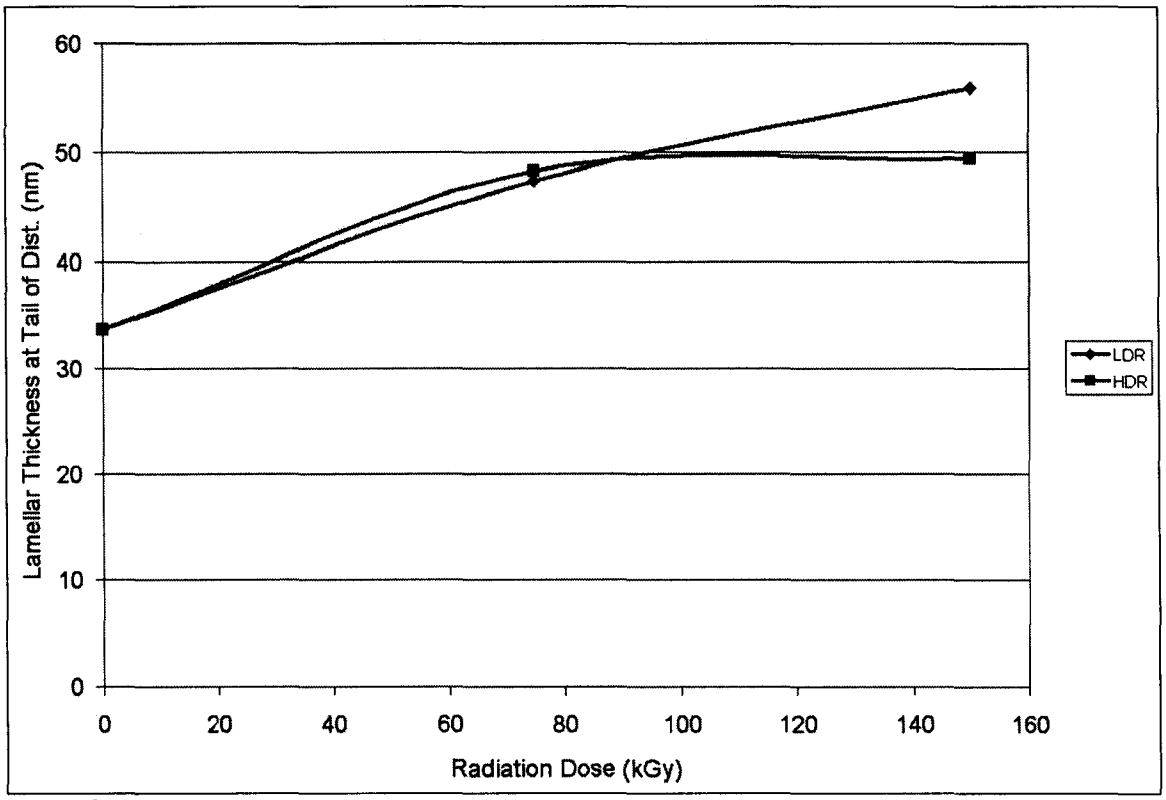

Figure 8

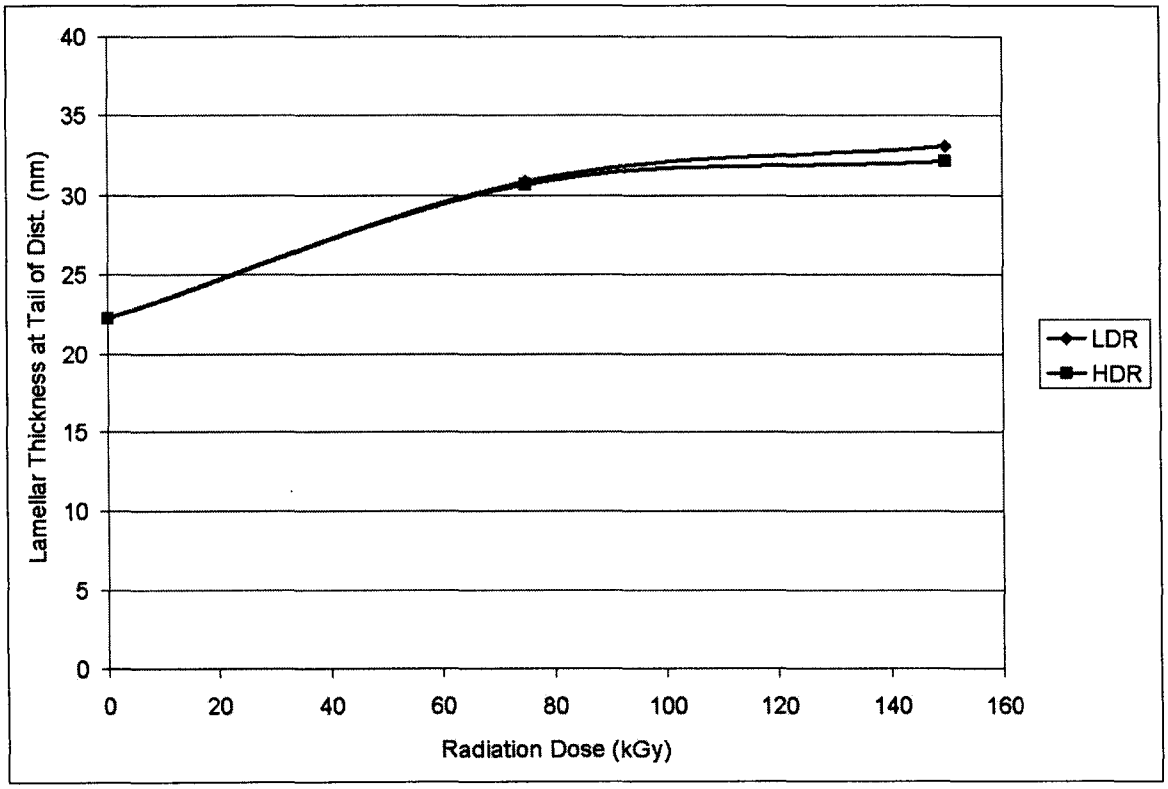

Figure 9

Table 2

Sample		Crystal 1	Crystal 2
Control	Top	11.746	31.167
	Middle	11.372	30.068
75 kGy HDR	Top	12.202	33.319
	Middle	11.902	32.181
75 kGy LDR	Top	10.479	28.818
	Middle	11.848	31.737
150 kGy HDR	Top	12.629	35.703
	Middle	12.216	32.28
150 kGy LDR	Top	11.55	33.605
	Middle	11.315	31.187

Kuebeckgasse - layout of apartment

bed: 1 m width/ 2 m length

couch: can be pulled out for two persons - cable TV, telephone and internet can be added if wanted

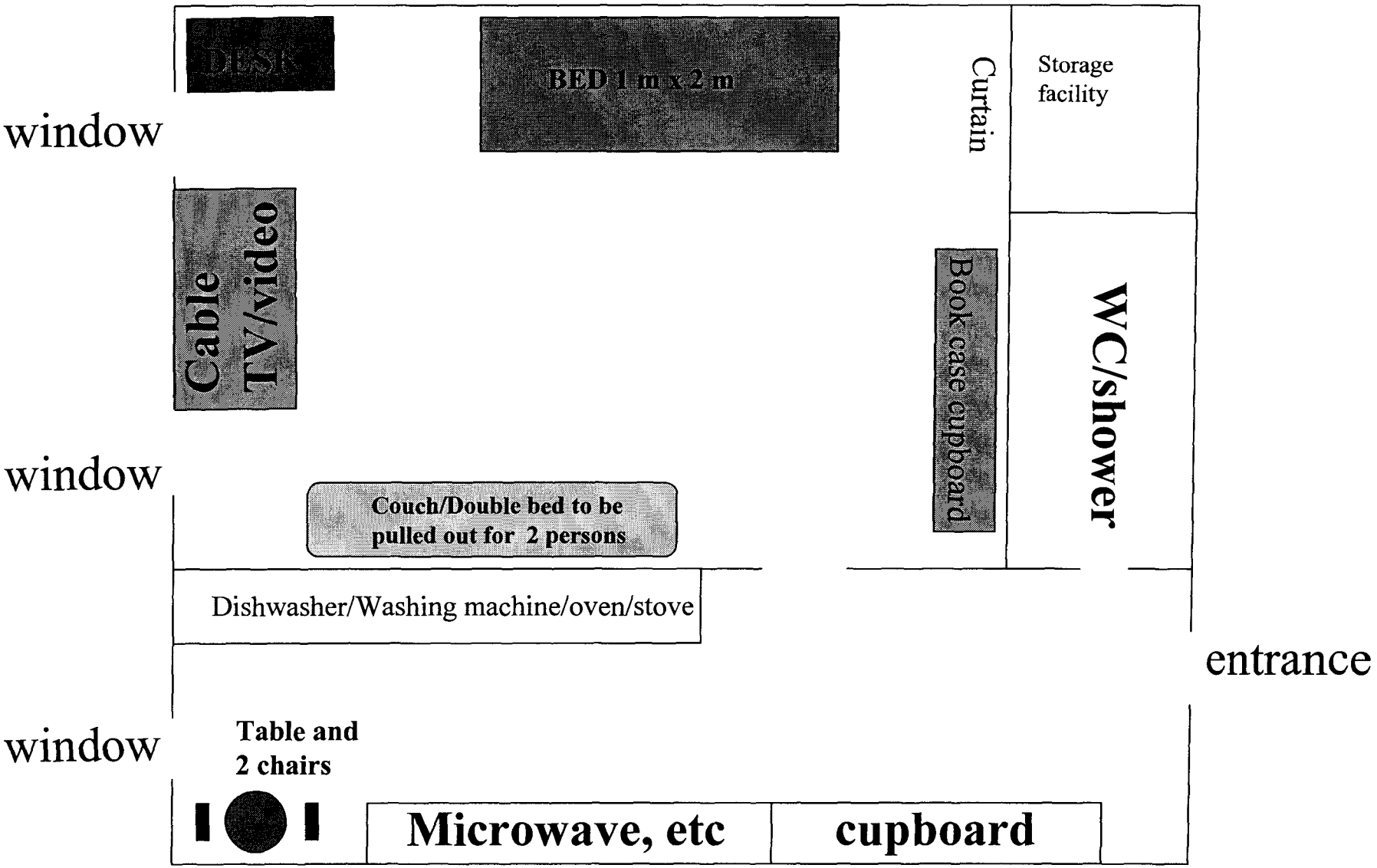

also poster for URCA

Senior Project
Approval & Completion Form

To be submitted on the **last day for providing the semester grades** and forwarded to:

University Honors Program, F 101 Melrose Hall
Tel.: 974-7875
Fax: 974-4352
honors@utk.edu

Student		**Faculty**	
Name	: Ann-Haley White	Name	: MATTHEW T. THERIOT
Major	: Social Work	Discipline	: SOCIAL WORK
ID	: 413-45-8020	Rank	: ASSISTANT PROF.
E-mail	: kwhite1@utk.edu	E-mail	: mtheriot@utk.edu
Phone	: 330-9951	Phone	: 4-8109

Project
Title : DISTRESS AND LIFE PROBLEMS IN CANCER PATIENTS: IDENTIFYING AREAS FOR INTERVENTION

Approval

☒ I have reviewed this completed senior honors project with this student and certify that it is complete and commensurate with honors level undergraduate research in the field.

☒ Based on its academic merits, I recommend that this project be digitally catalogued and archived by Hodges Library to make it widely available.

☒ I recommend this project for an Award of Distinction.
Note: A small number of awards, including financial recognition, will be given at the UHP spring convocation.

Faculty Member's Signature — Date: 4-4-05

☐ Read, approved and recorded

University Honors Program — Date

(November 2004)

Distress and Life Problems in Cancer Patients: Identifying Areas for Intervention

Ann-Haley White
The University of Tennessee
College of Social Work

Introduction

- Distress is a common response to cancer and other medical conditions.
- Distress interferes with patients' ability to cope effectively with the physical and emotional impact of disease.
- Research identifying specific problems confronting distressed patients will direct and inform social work practice.

Research Question

- What specific problem areas are associated with high levels of reported distress in patients awaiting diagnoses at a cancer treatment facility?

Methods

- N = 73
- Data collected as part of intake interview at one cancer treatment facility.
- Distress measured on 11-point self-report National Comprehensive Cancer Network scale (0 = no distress; 10 = extreme distress)
- Life problems experienced in past week measured on 35-item checklist scale (Alpha = .8869) with 3 subscales:
  1. Physical Problems (20 items; Alpha = .8768)
  2. Emotional Problems (5 items; Alpha = .7447)
  3. Family/Spiritual Problems (10 items; Alpha = .6320)
- Data analyzed using Independent-samples T-tests.

Sample Characteristics (N = 73)

- Gender: 54 Females (73.9%)
- Ethnicity: 62 Caucasian (84.9%)
- Marital Status: 42 Married (57.5%)
- Mean Age: 54.99 years (S.D. = 16.56)
- Have Medicare Insurance: 22 (30.1%)

Distress and Life Problems Results (N = 56)

Instrument	Mean	Standard Deviation
Distress Scale	4.64	3.26
Life Problems Checklist	5.62	5.45
Physical Problems Subscale	2.88	3.66
Emotional Problems Subscale	1.90	1.66
Family/Spiritual Problems Subscale	0.84	1.34

Mean Scores by Level of Distress

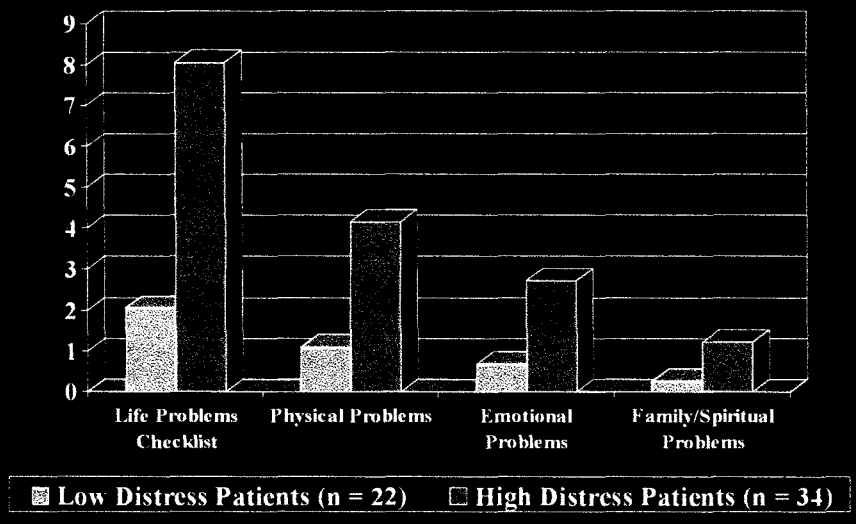

T-Test Comparisons of High and Low Distress Patients (N = 56)

Low Distress Patients (score 0-4): 22 (39.3%)
High Distress Patients (score 5-10): 34 (60.7%)

- Life Problems Checklist: T = -5.32, df = 52, p < .001
- Physical Problems Subscale: T = -3.73, df = 52, p < .001
- Emotional Problems Subscale: T = -5.85, df = 54, p < .001
- Family/Spiritual Problems Subscale: T = -3.08, df = 50, p = .003

Conclusions

- High distress patients report significantly more life problems overall.
- High distress patients report significantly more problems on all 3 subscales.
- No differences in level of distress by gender or marital status.
- No differences in reported life problems by gender or marital status.

Discussion

- High distress might indicate numerous life problems beyond patients' immediate medical concerns.
- Social workers should assess patients' social, emotional, and medical needs.
- High distress patients require an holistic approach to medical and social work care.

Limitations

- Inconsistent staff cooperation and participation
- Small number of data collection instruments
- Lack of ethnic diversity

Future Research

- Longitudinal research of changes in distress levels throughout diagnostic and treatment processes.
- Qualitative interviews with patients and their support system.
- Evaluate effectiveness of interventions to decrease distress levels and life problems.